Geophys. J. R. astr. Soc. (1980) **63**, 747–758

A slowness approach to the reflectivity method of seismogram synthesis

Gerard J. Fryer* *Hawaii Institute of Geophysics, 2525 Correa Road, Honolulu, Hawaii 96822, USA*

Received 1980 April 1; in original form 1980 January 7

Summary. Of the many schemes available for computing synthetic seismograms, the reflectivity method is probably the most widely used because of its ability to provide complete solutions. The method does, however, suffer the disadvantage that intermediate results are quite difficult to interpret. A new reflectivity technique, here called reflectivity-slowness, results if the original method is reformulated using a slowness rather than a spectral approach. The new procedure bears a strong similarity to the WKBJ method, but retains the ability to give complete solutions. The reflectivity-slowness and WKBJ methods share the property that intermediate results are readily interpreted; this feature may eventually be exploited in the solution of the inverse problem.

Introduction

The reflectivity method for the computation of synthetic seismograms (Fuchs & Müller 1971) is widely used as an aid to the interpretation of body-wave seismograms, especially in lithospheric studies. The method does, however, suffer two major disadvantages. The first is expense. The technique involves the computation of a reflectivity function and the double transformation of that function from frequency–wavenumber to time–distance space. The reflectivity function must be adequately sampled to avoid aliasing on transformation, so that a very large number of reflectivity computations are required. Determination of reflectivities involves solution of a differential equation for the depth-dependent part of the wave equation, which, even for very simple problems, implies numerical solution. The transforms too are evaluated numerically, so every stage of the synthesis is inherently expensive. The second disadvantage is more profound. The early recourse to numerical analysis means that intermediate results are complicated and difficult to interpret. Since synthetics are used primarily as a guide to the solution of the inverse problem, this complication is unfortunate; it forces model improvements to be made essentially by trial and error. One method for the computation of theoretical seismograms does not suffer the problem of complexity or expense: the WKBJ method (Chapman 1978; Dey-Sarkar & Chapman 1978). The WKBJ method is approximate, however, so it is most useful for the initial iterations of an inversion process. Because it is the most exact of the methods available, the reflectivity method should

* Present address: Department of Geological & Geophysical Sciences, Princeton University, Princeton, New Jersey 08544, USA.

be used to verify the final models, especially if structures are complicated by high velocity gradients or low velocity zones (Burdick & Orcutt 1979). Any reformulation of the reflectivity technique which would reduce expense or allow a simpler interpretation of intermediate results would obviously be worthwhile.

Any seismogram synthesis technique involves operations equivalent to those in the reflectivity method: solution of a differential equation followed by two inverse transformations which are essentially an integration with respect to frequency and one with respect to wavenumber (or equivalently to wave-slowness). The two transformations may be performed in either order separating synthesis techniques into the two classes identified by Chapman (1978). A spectral method is one in which the wave-slowness integral is evaluated first; the alternative, initial evaluation of the frequency integral, is called a slowness method. The reflectivity method is the best known of the spectral methods, but it can be reformulated using the slowness approach. That reformulation is the subject of this paper. I shall refer to the reformulated technique as the reflectivity-slowness method and illustrate its use by considering a simple example. It will become apparent that the chief advantage of the new method is that intermediate results are much simpler to interpret.

General theory

The reflectivity method of Fuchs & Müller (1971) is a scheme for computing the response of a layered half-space to a near-surface point source. In order to reduce computation time the complete response is computed only for the lower part of the structure, called the 'reflection zone'. For shallower layers (which are of lesser interest), only transmission losses and time delays are considered. We shall use the same approach here, but for simplicity we shall consider only a single fluid (ocean) layer overlying the reflection zone. For more complicated shallow structures the generalizations of Fuchs & Müller (1971) and Kennett (1975) may readily be incorporated into this method.

The geometry of the problem is shown in Fig. 1. The structure consists of a water layer of depth h and uniform sound velocity α_0. The reflection zone begins at the ocean bottom and includes all deeper structure. We consider a receiver at a depth z from the surface a horizontal distance r from an explosive source with a displacement potential time function $s(t)$. The Fourier transformed displacement potential for energy returned from the ocean bottom (i.e. from the reflection zone) will be

$$\hat{\phi}(r, z, \omega) = \hat{s}(\omega) \int_0^\infty (k/i\nu_0) R_{pp}(\omega, k) J_0(kr) \exp\left[i\nu_0(2h - z)\right] dk, \tag{1}$$

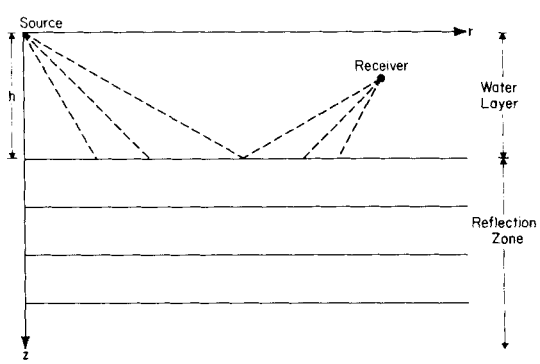

Figure 1. The problem considered. The response of a layered half-space (the reflection zone) to a point source at the surface of an overlying water layer is to be synthesized. Direct and surface reflected phases are ignored.

where R_{pp} is the P–P reflection coefficient at the ocean bottom, k is the horizontal wavenumber and ν_0 is the vertical wavenumber in the water (medium zero) given by

$$\nu_0^2 = (\omega/\alpha_0)^2 - k^2.$$

The reflectivity function R_{pp} includes all multiple reflections and interconversions of wave types within the reflection zone. It is usually computed using one of the more efficient matrix methods such as the phase-related approach of Kennett (1974).

Equation (1) is consistent with the following definition of the Fourier transform pair

$$\hat{\phi}(\omega) = \int_{-\infty}^{\infty} \phi(t) \exp(i\omega t)\, dt,$$

$$\phi(t) = \frac{1}{2\pi} \int_{-\infty}^{\infty} \hat{\phi}(\omega) \exp(-i\omega t)\, d\omega.$$

As Chapman (1978), we have denoted the Fourier transform of $\phi(t)$ by $\hat{\phi}(\omega)$.

From equation (1) the vertical displacement, w, is obtained by taking the derivative with respect to depth z. This gives

$$\hat{w}(r, z, \omega) = -\hat{s}(\omega) \int_0^{\infty} R_{pp}(\omega, k) J_0(kr) \exp[i\nu_0(2h - z)]\, k\, dk.$$

Making the substitution $k = \omega p$ we obtain the slowness integral

$$\hat{w}(r, z, \omega) = -\hat{s}(\omega) \int_0^{\infty} R_{pp}(\omega, p) J_0(\omega p r) \exp[i\nu_0(2h - z)]\, \omega^2 p\, dp, \tag{2}$$

where p is the horizontal slowness and q is the vertical slowness given by

$$q^2 = \alpha_0^{-2} - p^2.$$

The desired time function is the inverse Fourier transform of equation (2)

$$\hat{w}(r, z, t) = -\frac{1}{2\pi} \int_{-\infty}^{\infty} \int_0^{\infty} \hat{s}(\omega) \omega^2 R_{pp}(\omega, p) J_0(\omega p r) \exp\{i\omega[q(2h - z) - t]\}\, p\, dp\, d\omega. \tag{3}$$

In the original reflectivity method, the slowness integral in equation (3) (a Hankel transform) is evaluated numerically for each frequency at a desired range r. This results in a frequency series which is inverse Fourier transformed to give a time series, which when convolved with an appropriate source function yields the desired synthetic. If the order of the two transforms is interchanged, intermediate results are time series for particular values of slowness. These time series may be integrated numerically to give a time series at a particular distance. This alternate method is the slowness method.

THE SLOWNESS METHOD

We choose here to evaluate the Fourier transform in equation (3) before the Hankel transform. Changing the order of integration and applying the fundamental theorems of Fourier transformation (Bracewell 1965, p. 122), we get

$$w(r, z, t) = \frac{1}{r} \frac{d^2}{dt^2} \int_0^{\infty} \{s(t) * \check{J}_0(t/pr) * \check{R}_{pp}[t - q(2h - z), p]\}\, dp \tag{4}$$

where the star, *, denotes convolution in the time domain. $\check{J}_0$ and $\check{R}_{pp}$ are the inverse Fourier transforms of the Bessel function J_0 and the reflectivity R_{pp}. Notice that while the original slowness integral of equation (2) involved a complex exponential and the complex function R_{pp}, the Fourier transformed version (equation 4) involves only real functions. The transformed reflectivity, $\check{R}_{pp}$, is real since the original function R_{pp} is Hermitian (i.e. $R_{pp}(\omega, p) = R^*_{pp}(-\omega, p)$). Hence, by Fourier transformation, the complex arithmetic of the original method has been eliminated and all subsequent computation involves only real quantities. However, this does not imply that the slowness approach has any intrinsic computational superiority over the spectral approach; if the complex R_{pp} has been computed for $n/2$ frequencies, then the real $\check{R}_{pp}$ is defined for n times, so the total amount of computation required is identical in either method.

If the range r is large enough that the wavefronts are approximately planar, equation (4) can be simplified by using the far-field approximation for $\check{J}_0$ given by Chapman (1978),

$$\check{J}_0(t) \simeq \frac{1}{2^{1/2}\pi}\left\{\frac{H(1-t)}{(1-t)^{1/2}} + \frac{H(t+1)}{(t+1)^{1/2}}\right\},$$

where $H(t)$ is the Heaviside step function. Using this approximation,

$$\check{J}_0(t/pr) \simeq \left(\frac{pr}{2}\right)^{1/2} \frac{1}{\pi}\left\{\frac{H(pr-t)}{(pr-t)^{1/2}} + \frac{H(t+pr)}{(t+pr)^{1/2}}\right\}.$$

The first term in parentheses represents a disturbance travelling with positive phase velocity; the second term, negative phase velocity. For body waves in the far field the second term will yield negligible contribution to the slowness integral. We ignore the second term and use

$$\check{J}_0(t/pr) \simeq \left(\frac{pr}{2}\right)^{1/2} \frac{1}{\pi} \frac{H(pr-t)}{(pr-t)^{1/2}}. \tag{5}$$

Substituting the approximation (5) into equation (4), readjusting time lags, and making use of the properties of the derivative of a convolution (Bracewell 1965, p. 118), we obtain

$$w(r, z, t) = \pi^{-1}(2r)^{-1/2}\ddot{s}(t) * \lambda(-t) * \int_0^\infty p^{1/2}\check{R}_{pp}(t - t_0, p)\, dp, \tag{6}$$

where, for convenience, we have defined the function $\lambda(t) = H(t)t^{-1/2}$ and where t_0 is the time delay

$$t_0 = pr + q(2h - z).$$

If $\lambda(t)$ is time-reversed it becomes its Hilbert transform, which we shall denote by an overbar, hence $\lambda(-t) = \bar{\lambda}(t)$. This Hilbert transformation can be moved to any convenient term in the convolutions of equation (6) since Hilbert-transformed convolutions have the property that

$$\overline{f * g} = \bar{f} * g = f * \bar{g}.$$

Since Hilbert transformation just involves a $\pi/2$ change in the phase of spectral components, it is conveniently combined with Fourier transformation. We therefore choose to rewrite equation (6)

$$w(r, z, t) = \pi^{-1}(2r)^{-1/2}\ddot{s}(t) * \lambda(t) * \int_0^\infty p^{1/2}\bar{\check{R}}_{pp}(t - t_0, p)\, dp, \tag{7}$$

which has the same form as equation (30) of Chapman (1978).

At this point it is worth expanding on the meaning of $\check{R}_{pp}$. The reflectivity $R_{pp}(\omega, p)$ is a plane wave function, as is readily apparent from equation (3). This means that for any particular slowness p, the inverse transform of R_{pp}, the time series $\check{R}_{pp}(t, p)$, is the response of the structure to an impulsive plane wave of that slowness. Phinney, Chowdhury & Frazer (1980) suggest that such time series be referred to as plane wave seismograms. We shall refer to the complete function $\check{R}_{pp}$ for all slowness as the plane wave response.

The original reflectivity function is computed without any consideration of source–receiver geometry. The Fourier transformation converts the frequency dependence to a time dependence, but the only time that can be defined for the ocean bottom (or any surface) without specifying source and receiver separation is intercept time $\tau = t - pr$. Hence the time dependence of $\check{R}_{pp}$ is intercept time at the ocean bottom. For the problem being considered, however, the source and receiver are not at the ocean bottom but some distance above it. As a result, the time argument of $\check{R}_{pp}$ in equation (7) is not $t - pr$ but $t - pr - q(2h - z)$. The additional term $q(2h - z)$ is the total travel time of a disturbance in the water and must be subtracted to account for source–receiver geometry. If more than one layer were included in the region above the reflection zone, as in the original treatment of Fuchs & Müller (1971), additional time delay terms would appear in equation (7).

For a more direct comparison with the original reflectivity method, integration over slowness can be replaced by integration over angle. Let γ be the angle of incidence at the top of the reflection zone so that $\gamma = \sin^{-1}(p\alpha_0)$. Changing the variable of integration in equation (7) to γ leads to

$$w(r, z, t) = (2r\pi^2\alpha_0^3)^{-1/2}\,\ddot{s}(t) * \lambda(t) * \int_0^{\pi/2} \sin^{1/2}(\gamma)\cos(\gamma)\ddot{\check{R}}_{pp}(t - t_0, \gamma)\,d\gamma, \tag{8}$$

where the time delay t_0 is

$$t_0 = pr + q(2h - z) = [r\sin\gamma + (2h - z)\cos\gamma]/\alpha_0. \tag{9}$$

In equation (8) the integration has been limited to real angles of incidence. For body waves at sufficiently large range, truncating the integration at $\gamma = \pi/2$ leads to negligible error, but for surface waves or at close range the integration must be extended to complex angles of incidence (Stephen 1977).

Numerical approach – a simple example

To compute synthetics using an expression of form similar to equation (7), Chapman (1978) suggests using the WKBJ approximation to solve the p integral. However, to retain generality and to compute synthetics for situations where the WKBJ approach is difficult to apply or is inappropriate, we choose to evaluate the integral numerically. The most obvious procedure is to compute the reflectivity function R_{pp}, transform to get $\ddot{\check{R}}_{pp}$, perform the p integrations at a series of times for a given range, and finally obtain a synthetic seismogram by convolving with the 'effective source' $s(t) * \lambda(t)$. However, poorly defined dc levels and singularities in $\check{R}_{pp}$ make the numerical integration rather noisy and unstable, so the obvious procedure has to be modified somewhat. The exact nature of such problems and the means of their solution are most readily explained using an example.

We shall consider the simple structure shown in Table 1 and describe how the slowness approach can be used to synthesize the vertical motion at the surface arising from a surface point source. The structure consists of a 5 km deep homogeneous water layer, 1 km of homogeneous sediments and an homogeneous basement. We choose to ignore the direct and surface-reflected phases, and to model only energy return from the ocean bottom. It is

Table 1. A simple test model.

Layer thickness (km)	P velocity (km s^{-1})	S velocity (km s^{-1})	Density	P wave Q	S wave Q
5.0	1.50	–	1.03	∞	–
1.0	2.0	1.0	1.7	200	20
∞	4.0	2.0	2.5	500	167

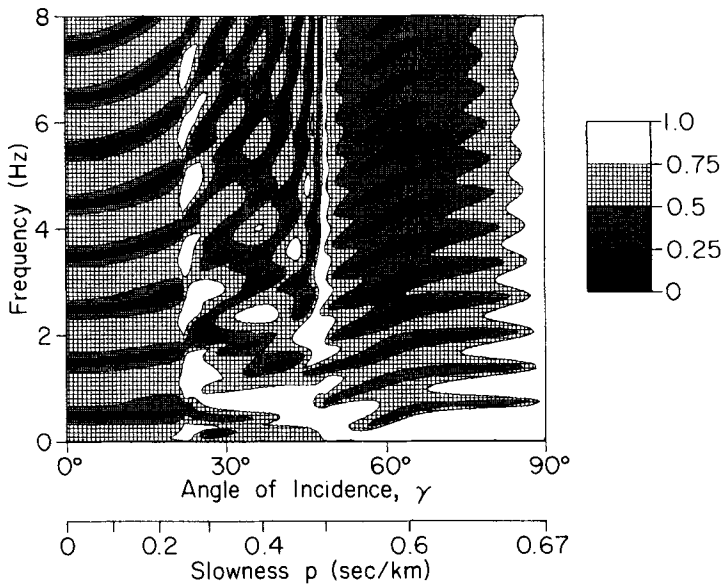

Figure 2. Modulus of the ocean bottom reflectivity function R_{pp} for the structure of Table 1.

natural then to specify the top of the reflection zone as the water–sediment interface. The plane-wave reflectivity function R_{pp} for this structure was computed for frequencies from 0.0625 to 8 Hz and for angles from normal to grazing incidence on the bottom at increments of half a degree. This computation was performed using Kind's (1976) algorithm, modified to include attenuation and to handle the fluid–solid boundary (Fryer 1978). Any equivalent procedure could have been used.

The modulus of the reflectivity function is shown in Fig. 2. The function is dominated by interference features. From normal incidence to 22° the interference fringes are primarily caused by compressional waves in the sediment. At 22°, compressional waves are critically incident at basement, resulting in a frequency-independent ridge. A similar ridge exists at 46° where compressional waves are critically reflected from the sediment and shear waves from the basement. Between these two angles is a complex region of interconversion and resonance. Beyond 46° interference fringes arise from P–S conversion at the sediment–water interface and shear resonance within the sedimentary layer. The fringes decay rapidly with increasing frequency because of the low value (20) specified for shear wave Q.

THE INVERSE FOURIER TRANSFORM

If $R_{pp}(\omega, \gamma)$ is inverse Fourier transformed with respect to frequency we obtain the plane wave response $\check{R}_{pp}(t, \gamma)$. Since the transform is of finite length, the usual problems of edge

effects and side-lobes arise, so smoothing is necessary for the subsequent integration over angle to be stable. For this work smoothing was done in the frequency domain before transformation using a cosine-squared function tapering to zero at the Nyquist (although any gentle taper would have been adequate). In Chapman's WKBJ approach an equivalent smoothing is required (Dey-Sarkar & Chapman 1978). Part of the smoothed plane-wave response is plotted in Fig. 3. An explanation of those arrivals for which a simple ray

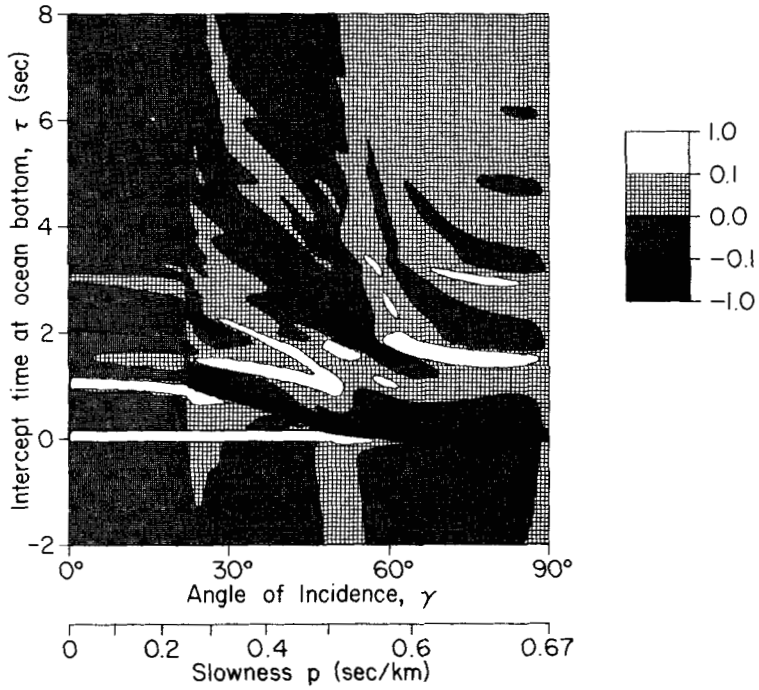

Figure 3. The plane wave response R_{pp}. Units are arbitrary.

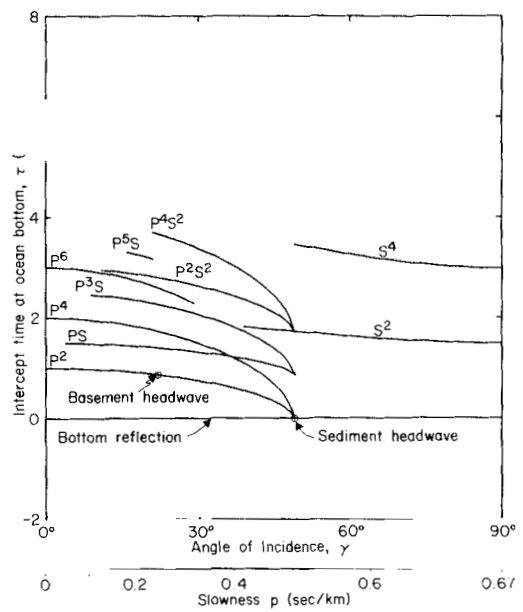

Figure 4. A ray interpretation of Fig. 3; see text for explanation.

interpretation is possible is shown in Fig. 4. In Fig. 4 each kinematic group is identified by the type and number of passages through the sediment layer; thus P^3S represents all rays that make three passages as compressional waves and one passage as shear. The plane-wave response (Fig. 3) is as expected; first reflections are positive when they are subcritical, change rapidly in phase at the appropriate critical angle, and become negative for supercritical incidence. Multiples have the appropriate sign changes. In the vicinity of the critical angles at 22° and 46°, low amplitude precursors are apparent, these are a result of the phase change of arrivals near critical incidence, as described by Arons & Yennie (1950).

Since it is necessary for the plane wave response to be smoothed before further analysis, it is most economical to perform the convolution with the source function at the same time. The smoothing and convolution can be combined into a single step equivalent to convolution with a smoothed source function. It is a common practice to include the source by specifying the function $\dot{s}(t)$ (e.g. Fuchs & Müller 1971; Dey-Sarkar & Chapman 1978). This is because compressional wave displacement in the far-field is proportional to the derivative of the source displacement potential. For this example, the compressional wave displacement, and hence $\dot{s}(t)$, was chosen to be a simple half-sinusoid of half a second duration and the convolution-smoothing operation was performed by multiplication in the frequency domain. In this particular case the source function was sufficiently band-limited that the smoothing was probably unnecessary. The result of the convolution is shown isometrically in Fig. 5, a plot of $\dot{s}(t)*\check{R}_{pp}(t, \gamma)$. Precursors at the critical angles are quite obvious in Fig. 5.

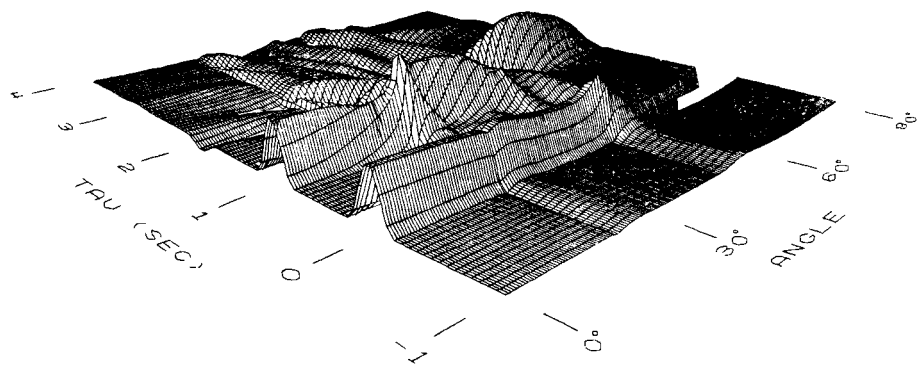

Figure 5. The plane wave response convolved with a half-sinusoid source function.

Because the reflectivity program used here could not compute zero frequency reflectivities, the lowest frequency used was 0.0625 Hz and zero frequency values were assumed to be zero. The time series obtained by inverse transformation of a frequency function with zero dc level must have a zero mean. However, a zero mean is likely to be inappropriate for a finite length time series as it may force the background level to be non-zero. For example, for the case considered here, the response near normal incidence is dominated by the positive bottom and basement reflections; since a zero dc level implies a zero mean, the whole of the rest of the response is mildly negative, as is apparent from 0 to 20° in Fig. 3. In any practical application of seismogram synthesis the lowest frequency used should not have to be any lower than the lowest frequency present in the source function, but ignoring lower frequencies can lead to slow, angle-dependent variation in the zero-level of the plane wave response. If the source function used does not have zero mean, this zero-level variation will introduce noise into the angle integration and give anomalous amplitudes for weak

arrivals such as head waves. However, the problem is readily solved. Equation (8) shows that an additional time derivative is required in computing the synthetic. Since differentiation is a form of high-pass filtering, the zero offset is suppressed and the problem bypassed if the reflection response is differentiated before the angle integration.

As with the smoothing and source convolution operations, taking the derivative is most readily accomplished in the frequency domain before taking the initial transform (this is done simply by multiplying by $-i\omega$). We note from equation (10) that Hilbert transformation is also required, this is equivalent to multiplying the frequency function by $-i\,\mathrm{sgn}\,(\omega)$. The two operations can obviously be combined by multiplying by $-|\omega|$. The final result is the function

$$W(t, \gamma) = \ddot{s}(t) * \tilde{\tilde{R}}_{pp}(t, \gamma),$$

which is plotted in Fig. 6. It is apparent that despite the additional derivative, the surface W is smooth enough for the Hankel transformation to be evaluated by numerical integration. Note also that the 'non-causal' precursors have been suppressed.

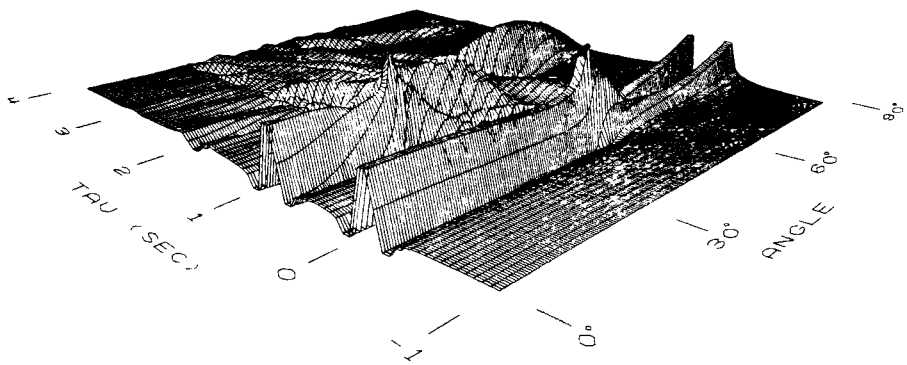

Figure 6. The function $W(t, \gamma)$ of equation (10). This is the Hilbert transformed time derivative of Fig. 5.

THE INVERSE HANKEL TRANSFORM

Once the function W of equation (10) has been obtained we wish to perform the inverse Hankel transformation by evaluating the angle integral from equation (8),

$$G(r, z, t) = \int_0^{\pi/2} \sin^{1/2}\gamma \cos\gamma\, W(t - t_0, \gamma)\, d\gamma \tag{11}$$

or the equivalent slowness integral from equation (7). The desired seismogram is then given by

$$w(r, z, t) = (2r\pi^2\alpha_0^3)^{-1/2}\lambda(t) * G(r, z, t). \tag{12}$$

The function $W(t, \gamma)$ is defined only on equally spaced grid points, so interpolation will be required to obtain values along the desired integration paths. Because source and receiver are not on the reflecting surface (the ocean bottom), the integration paths are not the straight lines that they are in Chapman's (1978) work, but follow curved trajectories across the W landscape. These curves are dependent on the source–receiver geometry and are defined by the delay time function $t_0 = t_0(r, z, \gamma)$ given in equation (9). For simplicity, for the rest of this paper, we shall assume that source and receiver are at the surface ($z = 0$).

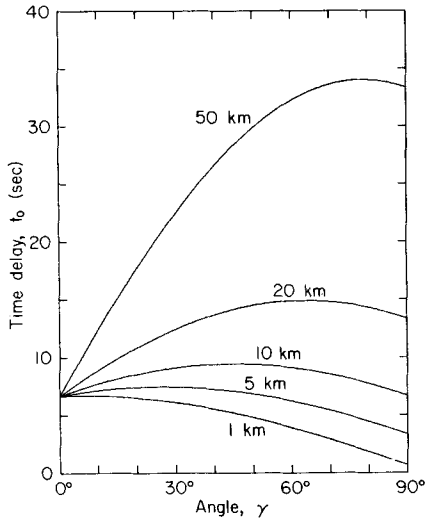

Figure 7. The time delay function t_0 for various ranges.

For a 5 km deep ocean, t_0 then has the angle dependence shown in Fig. 7 for various values of range, r. For normal incidence the time delay is the vertical two-way travel time through the water layer, while its maximum for any range occurs at the appropriate angle for specular reflection off the ocean bottom. Hence, at a range of 10 km, t_0 is a maximum at 45°, the expected angle for a 5 km deep ocean.

To compute a synthetic for a particular range r', the time series $G(r', 0, t)$ must be obtained by evaluating the integral (11) for the range of times of interest. The integral can be evaluated separately for each time, but this involves retrieval of information from the tabulated $W(t, \gamma)$ in a pseudo-transpose order and is extremely slow on a virtual memory computer. A better method is to consider the total contribution to $G(r', 0, t)$ for all times at a particular angle γ', and then proceed to the next angle. This is done by computing $t_0(r', 0, \gamma')$, then linearly interpolating in time to obtain the series $W(t - t_0, \gamma')$ for the desired times $t = t_i$; $i = 1, 2, 3, \ldots, n$. Each term in this series is given the trigonometric weighting $\sin^{1/2}\gamma \cos\gamma$ and added to $G(r', 0, t_i)$; $i = 1, 2, 3, \ldots, n$, before proceeding to the next angle. If only half of the contribution from the limiting angles of the integration is taken, then this procedure amounts to a trapezoidal integration. As with the original reflectivity method (Fuchs & Müller 1971), the integration need include only that range of angles of interest in any problem.

The final step in computing seismograms is to perform the range-dependent weighting and convolution with $\lambda(t)$ shown in equation (12). Synthetics generated by using the rational approximation to $\lambda(t)$ given by Wiggins (1976) are shown in Fig. 8 with superposed travel times for the major phases. Wiggins' rational operator makes the convolution extremely rapid but is inaccurate for periods longer than about 100 times the sampling interval. Such long-period errors are of no consequence to the short period seismograms plotted here. The synthetics shown in Fig. 8 are indistinguishable from those obtained from the original reflectivity method. The only difference is in computation time; after computation of the reflectivities, the original method took about four times longer than the slowness method.

I should point out here that the Hankel transform was evaluated by integrating over angle rather than over slowness so that a direct comparison could be made with a spectral reflectivity program using the same form of integration (and using the same reflectivities). The

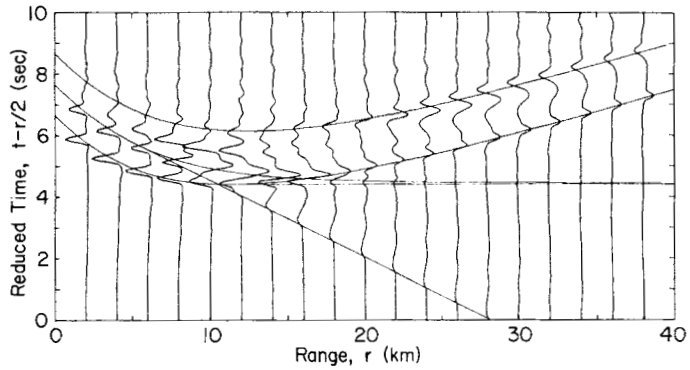

Figure 8. Seismograms and reduced travel times for the structure of Table 1.

change of variable from slowness to angle detracts somewhat from the elegance of the slowness approach and is awkward if the range of integration is to be extended to include surface waves. For all subsequent work using the reflectivity-slowness technique synthetics have been constructed using the slowness integration of equation (7) rather than the angle integration of equation (8).

Discussion

The reflectivity approach for computing synthetic seismograms is readily modified from a spectral to a slowness method. This modification was originally directed at reducing the expense of the reflectivity method, and indeed, considerable economies were realized. However, in retrospect, there is nothing in the mathematics which suggests the slowness method will be computationally superior. That the slowness approach was faster than the spectral is purely a consequence of superior code. The spectral program used, Kennett's (1975) modification of the original Fuchs & Müller (1971) program, has many options and broad application. Programs designed for specific problems always out-perform general programs, and that is exactly what happened here.

Where the slowness approach does hold an advantage over the spectral is in the manner of construction of the seismograms. Reflectivity-slowness shares this advantage with another important slowness method, the WKBJ technique (Chapman 1978). The WKBJ method is much more economical than the reflectivity method but may be inappropriate for complicated structures with high gradients or low velocity zones. Both slowness methods allow us to visualize a seismogram as the integrated cross-section of the plane-wave response. As shown by Figs 3 and 4, the plane-wave response is much more amenable to physical interpretation than the reflectivity function, so our physical comprehension of the synthesis process is improved. The plane wave response is also simpler to interpret than the final seismograms, as may readily be verified by comparing Figs 3 and 8. For example in τ–p space, reflections never cross in time and complications from interfering phases are greatly reduced. This would imply that it is better to analyse data and make comparison with models in τ–p space, a point which has important bearing on the inverse problem.

The most important recent advances in the inversion of seismic body wave data have come with the realization that travel time inversions are most effectively performed after transformation to τ–p space (Johnson & Gilbert 1972). This realization has resulted in a large number of inversion procedures for determining velocity–depth functions (e.g. Dorman 1979). However, such inversion schemes ignore amplitude information. The transformation of complete record sections to τ–p space seems a promising approach to an

inversion scheme which would include an assessment of amplitudes (Phinney *et al.* 1980), although problems such as source deconvolution and the limitations of finite data density have yet to be resolved (Chapman 1978). Since the slowness approach involves computation of synthetics from τ–p space it again appears that that is the space in which to compare model and data. If the comparison could be quantified in some manner this would be an important step forward in the development of a practical solution to the inverse problem.

A reviewer has made the observation that a more direct comparison of this and Chapman's (1978) work would result from absorbing the phase term $\exp(2i\nu_0 h)$ into R_{pp} in equation (1). The time dependence of $\check{R}_{pp}$ would then be the true intercept time for the source–receiver geometry used rather than the intercept time at the top of the reflection zone. Such an approach would be inconvenient for cases where the region above the reflection zone were laterally varying (making the phase term distance-dependent), but for the vast majority of applications combining the phase term with R_{pp} would be a worthwhile modification. Indeed, if source and receiver were at the same depth, the integration path for inverse Hankel transformation would then be a straight line in τ–p space, as it is in Chapman's treatment. This simplification of the integration path could probably be exploited to make the reflectivity-slowness approach more rapid. This is being investigated.

Acknowledgments

I thank George Sutton, Joe Gettrust and Neil Frazer for their critical comments. This study was supported by the Ocean Science and Technology Detachment of the Office of Naval Research.

This work forms part of a doctoral dissertation at the University of Hawaii. Hawaii Institute of Geophysics contribution number 1062.

References

Arons, A. B. & Yennie, D. R., 1950. Phase distortion of acoustic pulses obliquely reflected from a medium of higher sound velocity, *J. acoust. Soc. Am.*, **22**, 231–237.

Bracewell, R., 1965. *The Fourier Transform and its Applications*, McGraw-Hill, New York.

Burdick, L. J. & Orcutt, J. A., 1979. A comparison of the generalized ray and reflectivity methods of waveform synthesis, *Geophys. J. R. astr. Soc.*, **58**, 261–278.

Chapman, C. H., 1978. A new method for computing synthetic seismograms, *Geophys. J. R. astr. Soc.*, **54**, 481–518.

Dey-Sarkar, S. K. & Chapman, C. H., 1978. A simple method for the computation of body-wave seismograms, *Bull. seism. Soc. Am.*, **68**, 1577–1593.

Dorman, L. R., 1979. A linear relationship between Earth models and seismic body wave data, *Geophys. Res. Lett.*, **6**, 132–134.

Fryer, G. J., 1978. Reflectivity of the ocean bottom at low frequency, *J. acoust. Soc. Am.*, **63**, 35–42.

Fuchs, K. & Müller, G., 1971. Computation of synthetic seismograms with the reflectivity method and comparison with observations, *Geophys. J. R. astr. Soc.*, **23**, 417–433.

Johnson, L. E. & Gilbert, F., 1972. Inversion and inference for teleseismic ray data, *Meth. comput. Phys.*, **12**, 231–266.

Kennett, B. L. N., 1974. Reflections, rays and reverberations, *Bull. seism. Soc. Am.*, **64**, 1685–1696.

Kennett, B. L. N., 1975. Theoretical seismogram calculation for laterally varying crustal structures, *Geophys. J. R. astr. Soc.*, **42**, 579–589.

Kind, R., 1976. Computation of reflection coefficients for layered media, *J. Geophys.*, **42**, 191–200.

Phinney, R. A., Chowdhury, K. R. & Frazer, L. N., 1980. Transformation and analysis of record sections, *J. geophys. Res.*, in press.

Stephen, R. A., 1977. Synthetic seismograms for the case of the receiver within the reflectivity zone, *Geophys. J. R. astr. Soc.*, **51**, 169–181.

Wiggins, R. A., 1976. Body wave amplitude computations – II, *Geophys. J. R. astr. Soc.*, **46**, 1–10.